Lasing modes in equilateral-triangular laser cavities

H. C. Chang, G. Kioseoglou, E. H. Lee, J. Haetty, M. H. Na, Y. Xuan, H. Luo,* and A. Petrou
Department of Physics, State University of New York at Buffalo, Buffalo, New York 14260

A. N. Cartwright
Department of Electrical Engineering, State University of New York at Buffalo, Buffalo, New York 14260
(Received 26 August 1999; published 16 June 2000)

We report the study of lasing modes in broad-area, equilateral-triangular laser cavities. An alternative approach is proposed to study optical modes in equilateral triangular cavities in an analytical form. The modes were obtained by examining the simplest optical paths inside the cavity, which yields the final solution with the boundary conditions. The cavities can be fabricated from semiconductor heterostructures grown on (111)-oriented substrates, which can be easily cleaved into equilateral triangular shapes. Such a design takes advantage of total internal reflection at the cleaved facets of the cavity for circulating modes. Experimental results are obtained from cavities fabricated from a superlattice structure of $In_{0.13}Ga_{0.87}As/GaAs$ grown on a (111) GaAs substrate.

PACS number(s): 42.55.Px, 42.60.Da, 42.60.Jf

I. INTRODUCTION

Cleaved cavity semiconductor lasers are the simplest kind of laser structure because they are easy to fabricate and the cleaved facets have the highest degree of perfection. Thus they are widely used in commercial applications. Because of diverse performance needs, laser cavities of various shapes and dimensions have been intensely studied, including surface emitting lasers [1], microdisk lasers [2], micro-arc-ring lasers [3], triangular, L- and U-shaped ridge lasers [4–6], bow-tie lasers [7], and so on.

The purpose of this study is to investigate a cavity of triangular shape, taking advantage of the crystalline symmetries of the samples, namely those grown on (111) substrates, including GaAs- and GaN-based structures [8,9]. From a material point of view, samples grown on (111)-oriented substrates have shown excellent characteristics in the standard stripe laser geometry, which yield thresholds as low as 87 A/cm^2 [10].

Cavities of triangular shapes have been fabricated to explore possible advantages of such laser structures. However, the mode structure inside a triangular cavity has not been theoretically analyzed and used in actual laser designs. The focus of this paper is the optical modes in an equilateral triangular cavity. An analysis of the modes is needed for understanding the properties of lasing characteristics in this configuration. Although there have been studies on cavities in this configuration, the results were qualitatively interpreted [11,12]. The lack of calculated results also led to less-than-optimum designs in the past. In Ref. [11], for instance, waveguides are created as a part of the cavity for extracting the light beam from the cavity. Such waveguides, however, are created at the corners of the cavity where the light intensity is the lowest, as indicated by our calculations of normal modes. It should be pointed out that the cavities studied here are different from the ring lasers having an etched ridge along the side of the triangle [4].

Specifically, the configuration addressed here involves an equilateral triangular laser cavity in which the active medium covers the whole area of the triangle, cleaved from samples grown on (111) substrates. There are three cleavage planes perpendicular to (111), namely, $(10\bar{1})$, $(1\bar{1}0)$, and $(01\bar{1})$, which form equilateral triangles. The cavities reported here have each side of the triangles equal to or greater than 75 μm. Thus the optical modes can be calculated with the classical treatment of light waves for our purpose.

II. CAVITY NORMAL MODES

We will first examine the optical modes in an equilateral triangular cavity, whose electrical (and magnetic) component obeys the Maxwell equations in the well-known form

$$(\nabla^2 + \mu\varepsilon k^2)\psi = 0, \tag{1}$$

after the time variable is separated out [13], where ψ can be either the electric or magnetic field. The problem of this second-order partial differential equation in an equilateral triangle was treated a long time ago and refined subsequently [14]. In previous treatments, two wave vectors of the two-dimensional problem, $\mathbf{k}_1$ and $\mathbf{k}_2$, are parallel to two sides of the triangle (thus not orthogonal to each other) and periodic boundary conditions were used. Because the two wave vectors are not linearly independent, the results have terms involving $\mathbf{k}_1 \cdot \mathbf{k}_2$. Such terms obscure the physical picture of normal modes inside the resonant cavity. In order to analyze lasing action in such triangular cavities, it is critical to find normal modes having linearly independent wave vectors. In order to find solutions with two wave vectors perpendicular to each other, the coordinate system shown in Fig. 1 was used to calculate the two-dimensional problem (the x-y plane). The z direction, which is taken as the growth direction, is identical to other edge-emitting semiconductor lasers,

*Corresponding author.

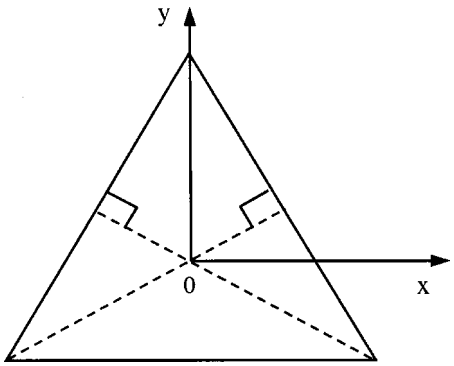

FIG. 1. The coordinate system used for the calculation of normal modes inside the triangular cavity.

and can be treated independently by separating z components of the differential equation from those involving x and y.

The magnitude of the electric field $E_z(x,y)$, which determines the intensity of the light traveling in the x-y plane, is expressed as a product of two parts having wave vectors *orthogonal* to each other, suitable to describe the normal modes. This choice, however, makes it impossible to solve the problem by variable separation because of the boundary conditions imposed by the threefold symmetry of the cavity. This is likely the reason why such a choice has never been used. As a result, a trial function has to be found, i.e., guessed, in order to solve the problem.

The purpose here is to examine if an equilateral triangular cavity has normal modes compatible with lasing action. For simplicity, we will show the result of a cavity with all facets having 100% reflectivity (i.e., the function vanishes at all three boundaries), as often used in such a situation, and corresponding to the TM mode. In this case, the problem can also be viewed as a particle in an infinite quantum well having the shape of an equilateral triangle. It is well known that normal modes in all systems with some degree of symmetry have the simplest and most symmetric form, which can often be rigorously identified even without unduly tedious calculations. This will be our guide to establishing the trial function for this problem. The simplest pattern in an equilateral triangle is the circulating path shown in Fig. 2(a), which includes the one that is reflected at the middle of all three sides as a special case. It can be seen that the segments of the path are always parallel to one of the sides. If one is to represent such a path in terms of plane waves, the wave function for the part of the path going in the positive x direction (parallel to the base of the triangle) can be simply expressed as e^{ik_1x}. Rotating this wave by 120° and 240° will result in the rest parts of the wave, respectively given by

$$e^{-ik_1[(x+a)/2-\sqrt{3}y/2]}, \quad e^{-ik_1[(x-a)/2+\sqrt{3}y/2]}, \tag{2}$$

where a is the side length of the triangle. These three plane waves can be used to represent the circulating wave shown in Fig. 2(a), with a wave vector k_1. Since the triangular cavity is a two-dimensional system, another wave vector has to be identified. As explained earlier, it is preferable to have k_1

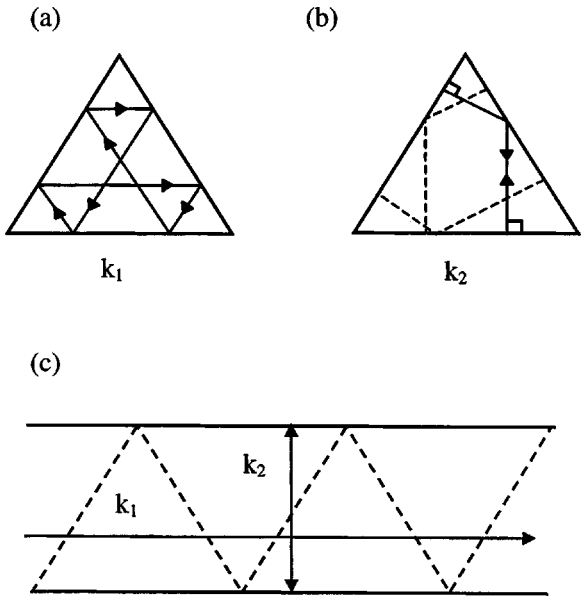

FIG. 2. Schematic diagrams of wave propagation inside the cavity: (a) clockwise traveling mode with wave vector $\mathbf{k}_1$, (b) the mode having wave vector $\mathbf{k}_2$ with each portion shown perpendicular to one part of the beam in (a), and (c) the equivalent picture of (a) and (b).

and k_2 perpendicular to each other for all segments of the wave. Following the same reasoning that normal modes should be simple, one finds that there is another group of paths, as shown in Fig. 2(b). This group of paths is in the form of standing waves, with normal incidence at two of the three sides and a 60° incident angle at the third side. As can be seen, each segment in this case is perpendicular to one of the three sides. For the part perpendicular to the base of the triangle, the wave can be written as $\sin(k_2y)$, where the sine function represents the *standing* aspect of the wave. This part is in fact perpendicular to e^{ik_1x}, which meets our requirement for the modes. By rotating this sine wave by 120° and 240°, one obtains the rest parts of the standing waves shown in Fig. 2(b) in the form of

$$\sin\left[k_2\left(\frac{\sqrt{3}}{2}x+\frac{1}{2}y-\frac{a}{2\sqrt{3}}\right)\right], \quad \sin\left[k_2\left(\frac{\sqrt{3}}{2}x-\frac{1}{2}y+\frac{a}{2\sqrt{3}}\right)\right], \tag{3}$$

respectively. Although it is less obvious than the two perpendicular waves just mentioned (one in the x direction and one in the y direction), the two standing waves in Eq. (3) are also respectively perpendicular to the two functions in Eq. (2). The next step is to multiply pairs of waves perpendicular to each other, $e^{ik_1x}\sin(k_2y)$, for example, resulting in a total of three terms. A linear superposition of the three terms with coefficients to be decided with the boundary conditions will give the trial function for this problem and has the following form:

$$E_z(x,y)=A\left\{ e^{ik_1x}\sin k_2\left(y+\frac{a}{2\sqrt{3}}\right)+Be^{-ik_1[(x+a)/2-\sqrt{3}y/2]}\times\sin\left[k_2\left(\frac{\sqrt{3}}{2}x+\frac{1}{2}y-\frac{a}{2\sqrt{3}}\right)\right]+Ce^{-ik_1[(x-a)/2+\sqrt{3}y/2]}\times\sin\left[k_2\left(\frac{\sqrt{3}}{2}x-\frac{1}{2}y+\frac{a}{2\sqrt{3}}\right)\right]\right\}. \tag{4}$$

The boundary conditions in this case can be written as

$$E_z(x,y)=0$$

$$\text{when } y=-\frac{a}{2\sqrt{3}},\quad y=-\sqrt{3}x+\frac{a}{\sqrt{3}},\quad y=\sqrt{3}x+\frac{a}{\sqrt{3}}. \tag{5}$$

In other words, $E_z(x,y)=0$ at all three sides of the triangle. By applying the boundary conditions to Eq. (4), we obtain

$$Be^{-ik_1(3a/4)}\sin\left[k_2\left(\frac{\sqrt{3}}{2}x-\frac{\sqrt{3}}{4}a\right)\right]+Ce^{ik_1(3a/4)}\sin\left[k_2\left(\frac{\sqrt{3}}{2}x+\frac{\sqrt{3}}{4}a\right)\right]=0, \tag{6}$$

$$\sin\left[k_2\left(-\sqrt{3}x+\frac{\sqrt{3}}{2}a\right)\right]+C\sin[k_2(\sqrt{3}x)]=0, \tag{7}$$

$$\sin\left[k_2\left(\sqrt{3}x+\frac{\sqrt{3}}{2}a\right)\right]+B\sin[k_2(\sqrt{3}x)]=0. \tag{8}$$

It is clear that Eqs. (6)–(8) are not simply algebraic equations involving the coefficients, as is usually the case for a problem of differential equations. Rather, x still remains in the equations after boundary conditions are applied. This originates from the fact that the problem cannot be solved by variable separation. By inspecting the equations, however, one realizes that the problem can be easily handled. If the sum of two sine functions is equal to 0, which is the case for Eqs. (6)–(8), the two functions have to be either ''in phase'' or ''out of phase,'' depending on the signs of the coefficients, B and C. From Eq. (6) this leads to

$$k_2\left(\frac{\sqrt{3}}{2}x-\frac{\sqrt{3}}{4}a\right)=k_2\left(\frac{\sqrt{3}}{2}x+\frac{\sqrt{3}}{4}a\right)+n\pi,\quad n=1,2,3\ldots, \tag{9}$$

which can be further simplified as

$$k_2=\frac{2n\pi}{\sqrt{3}a},\quad n=1,2,3\ldots. \tag{10}$$

This is in fact the solution for k_2. It is also easy to verify that this result is also valid for Eqs. (7) and (8). Substituting Eq. (10) back into Eqs. (6)–(8), we obtain

$$Be^{-ik_1(3a/4)}+Ce^{ik_1(3a/4)}(-1)^n=0, \tag{11}$$

$$1-C(-1)^n=0, \tag{12}$$

$$1+B(-1)^n=0. \tag{13}$$

Subtraction of Eq. (12) from Eq. (13) gives

$$B(-1)^n+C(-1)^n=0. \tag{14}$$

From Eq. (11) and Eq. (14), we have

$$\begin{vmatrix} e^{-ik_1(3a/4)} & e^{ik_1(3a/4)}(-1)^n \\ (-1)^n & (-1)^n \end{vmatrix}=0, \tag{15}$$

for a nonvanishing solution. It yields

$$k_1=\pm\frac{2m\pi}{3a},\quad m=1,2,3\ldots,\qquad B=(-1)^{n+1},\quad C=(-1)^n, \tag{16}$$

where m and n are both even or odd, and $n\neq m$. The eigenvalues and eigenfunctions appear to be quite different in form from those given in Ref. [14] because of the different choices of wave vectors. But the two sets of results are, however, equivalent. This is similar to the case of a charged particle in a magnetic field having different but equivalent solutions.

The two wave vectors calculated in our approach, $\mathbf{k}_1$ and $\mathbf{k}_2$, can be compared to the normal modes in a rectangular cavity. The wave vector $\mathbf{k}_1$ is always parallel to one of the three sides and represents clockwise and counterclockwise traveling waves, corresponding to the plus and the minus signs, respectively. This mode is shown in Fig. 2(a), and it is equivalent to the case shown in Fig. 2(c), in which the triangle is turned by 180° about the side where the beam is reflected. The only difference not shown in Fig. 2(c) is the fact that this wave travels periodically in the triangular cavity, which corresponds to an infinite length. The wave vector $\mathbf{k}_2$ corresponds to waves always perpendicular to one of the three sides of the triangle, illustrated in Fig. 2(b). The modes represented by $\mathbf{k}_1$ and $\mathbf{k}_2$ are similar to the longitudinal and lateral modes, respectively, in common rectangular cavities, except the longitudinal wave is a traveling wave rather than a standing wave in the rectangular cavity case. The round-trip lengths are $L_1=3a$ and $L_2=\sqrt{3}a$ for the longitudinal and the lateral modes, respectively.

It is important to point out that the mode related to $\mathbf{k}_1$, which corresponds to the propagating wave, experiences total internal reflection at all facets as long as the refractive index of the semiconductor is greater than 2.0, which is the case for all common semiconductors. Thus the [110] cleavage planes produce high quality mirrors not only because of their smoothness, but also the high reflectivity. This suggests that equilateral triangular cavities indeed constitute a very natural configuration to support lasing action. Furthermore, numerical calculations using the solution shown in Eq. (4) indicate that the light intensity drops much faster as it reaches the corners of the triangular cavities than when it

reaches the sides. The light should therefore be extracted from a side rather than from the corners as was done in Ref. [11], which can also been seen qualitatively in Fig. 2.

A question arises concerning the dominant mode in such a cavity. Two factors are of particular importance, namely, the reflectivity of the mirrors and the effective cavity length in connection to specific modes. It is easily seen that the longitudinal modes have higher reflectivity because they experience total internal reflection. The lateral modes have normal incidence at the mirrors and are expected to have substantially lower reflectivity if the mirrors are not coated. The results from the calculation show that the round-trip length for the longitudinal modes is longer than that for the lateral modes, indicating that the effective cavity length for the longitudinal modes is more favorable for lasing action. Thus the longitudinal mode is expected to be the dominant mode of the stimulated emission from such a cavity, as in rectangular cavities. In other words, the laser beam comes from the circulating modes associated with $\mathbf{k}_1$, consistent with our experimental results.

The intensity can be qualitatively viewed with $|E_z(x,y)|^2$, with the calculated values for k_1, k_2, B, and C. To illustrate the intensity distributions, two plots are shown in Fig. 3, with $|E_z(x,y)|^2$ proportional to the brightness, and black representing $|E_z(x,y)|^2=0$. Figure 3(a) shows the lowest lateral mode, i.e., $n=1$, and the 99th longitudinal mode ($m=99$)—a combination comparable to the experimental situations presented later, considering the emission wavelength and cavity size. The pattern shown in Fig. 3(b) has $n=2$ and $m=100$. The choice of m is to satisfy the requirement that n and m have to be both even or odd.

It should be pointed out that the solution given here is for the TM mode. The result is also valid for electronic states confined in a two-dimensional equilateral triangular quantum well with infinite barriers. This is because such a system will also be described by a second-order partial-differential equation and the boundary conditions are $\psi(x,y)=0$—$\psi(x,y)$ is the wave function and corresponds to $E_z(x,y)$ in our problem here—at all sides of the triangle.

III. EXPERIMENTAL RESULTS

The field intensity distribution of the beam along the growth direction is not directly affected by the triangular shape of the cavity. As for all other semiconductor lasers, the field distribution in this direction is determined by the light confinement in separate confinement structures and can be treated by conventional techniques. The samples used for this study are simple superlattice structures without the light confinement component. The waveguiding is realized with the difference of the average refractive index of the superlattice region and that of the buffer and cladding layers of the structure, which can be significantly improved with separate confinement laser structures.

To examine the feasibility of this configuration, equilateral triangular cavities were cleaved using GaAs-based structures. Because of the lack of ideal samples at the time of this study, we will present the results obtained using a simple $In_{0.13}Ga_{0.87}As/GaAs$ superlattice (SL) sample to demonstrate

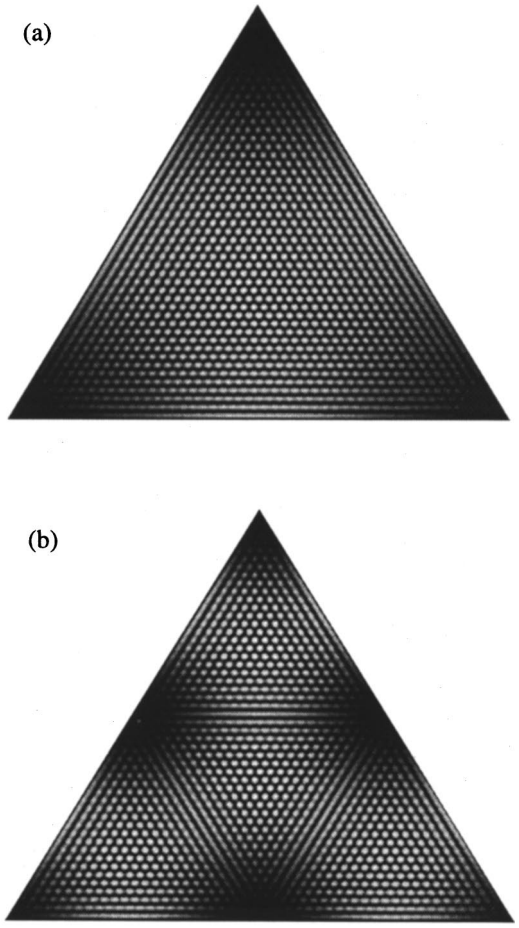

FIG. 3. Value of $|E_z(x,y)|^2$ inside the triangular cavity: (a) $m=99$, $n=1$, (b) $m=100$, $n=2$. The intensity is proportional to the brightness and black represents $|E_z(x,y)|^2=0$.

lasing action, which does not have separate confinement needed for better device performance. The sample was grown by molecular beam epitaxy on a GaAs(111)B substrate. A40 periods of 60 $In_{0.13}Ga_{0.87}As$/40 GaAs SL was grown between the GaAs buffer and cladding layers. The sample was cleaved along the (110) planes, which eliminates the complex processing steps used in lithography, while ensuring the high quality of the cavities. The side length of the equilateral triangular cavities fabricated for this study ranges from 75 to 350 μm.

Because the longitudinal mode propagating inside the cavity experiences total internal reflection at all facets, one of the facets has to be covered with a transparent material. The refractive index of this material should be greater than half of the value in the semiconductor, so that the wave can partially pass through. A transparent adhesive was used to cover one of the facets, such that the laser beam could exit the triangular cavity.

For lasing experiments, the samples were placed in a cryostat and optically pumped at low temperatures. Optical pumping was carried out by a pulsed nitrogen laser (pulse width ~3 ns, repetition rate 20 Hz) with an attached tunable dye module. The laser line used was at 555 nm, and the excitation beam entered the cavity from the top surface of the

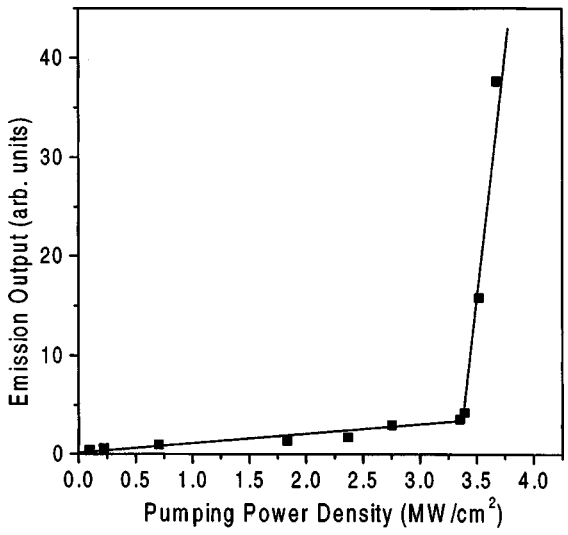

FIG. 4. Emission intensity from the triangular cavity laser as a function of pumping power density under pulsed excitation at $T = 10$ K. The solid line is a guide to the eye.

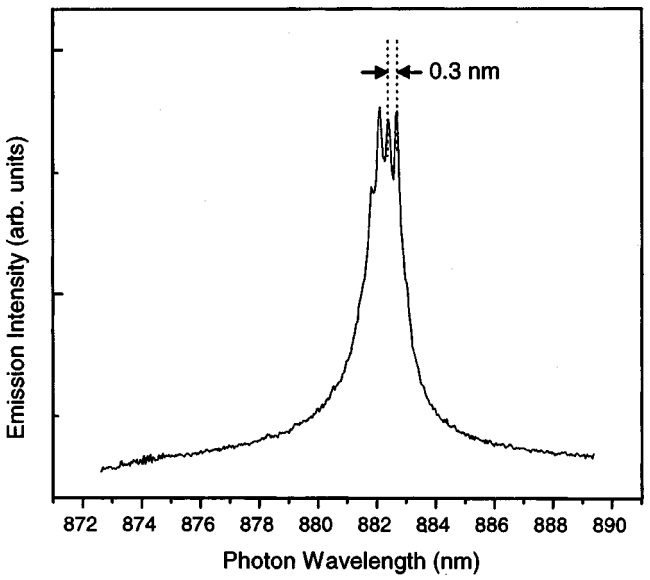

FIG. 5. The spectrum of multimode emission with an approximate mode spacing of 0.3 nm.

sample with near normal incidence. Edge emission through the transparent adhesive was scattered and the scattered signal was collected with a spectrometer.

The threshold behavior is shown in Fig. 4, in which the integrated emission intensity is plotted as a function of pumping power density at 10 K under pulsed operation. A threshold power density of 3.4 MW/cm^2 is estimated from this data. A multimode spectrum similar to those of stripe laser diodes is given in Fig. 5, showing the longitudinal modes. The separation between adjacent modes is $\Delta\lambda = 0.3$ nm for this particular sample.

From the mode spacing of the multimode emission spectra, we can estimate the round-trip length L of the stimulated emission inside the cavities and compare it to the dimensions of the cavities. This allows us to determine the mode of the lasing action as illustrated in Fig. 2. The length L is calculated with the following equation [15]:

$$L = \frac{\lambda^2}{[n - \lambda(dn/d\lambda)]\Delta\lambda} = \frac{\lambda^2}{\bar{n}\Delta\lambda}, \tag{17}$$

where we have used $\lambda = 880$ nm for the center lasing wavelength, and $\bar{n} = n - \lambda(dn/d\lambda) = 3.6$ for the effective refractive index of GaAs at 880 nm [16]. The results are given in Table I. From Table I, the round-trip lengths calculated using Eq. (17) match the round-trip lengths of longitudinal modes (the mode numbers for sample 1 in Table I, for example, are $m = 613$ and $n = 1$) within the error of measurement. This confirms the earlier assumption that the dominant mode inside the triangular cavity is the longitudinal mode, corresponding to k_1 in Eq. (4). This result contradicts the previous report, Ref. [12], in which the lateral mode was believed to be the dominant mode. Since there was no transparent layer deposited on the side of the cavity in Ref. [12] the circulating mode underwent totally internal reflection, and was mostly trapped inside the cavity. This could explain the discrepancy. The experimental results indicate single direction lasing under most of the conditions used. However, a clear understanding of mode competition requires a detailed analysis as a function of pumping conditions.

It should be pointed out that optical pumping was used and the threshold is very high at this stage, which can be expected from the superlattice structure, rather than a typical laser diode structure with separate confinement. Further studies will be performed with more suitable samples, so that the features of this configuration can be fully explored. Some nonlinear properties of broad-area lasers depend on sample geometry, such as filamentation. For the same far-field pattern due to filamentation, the carrier distribution inside the triangular cavity discussed here has to differ dramatically from that in a rectangular cavity. In other words, all nonlinear properties involving spatial charge distribution can be

TABLE I. A comparison of the round-trip lengths (discussed in the text) obtained from the measured cavity sizes and the lengths calculated from the mode spacings. The error for the measured cavity dimensions (using an optical microscope) is 5%.

Sample	Lateral round-trip length $\sqrt{3}a$ (μm)	Longitudinal round-trip length $3a$ (μm)	Calculated round-trip length L (μm)
1	312	540	546
2	440	765	738
3	285	495	514

expected to be different between triangular cavity lasers and the conventional edge-emitting lasers, which presents an interesting situation from the point of view of both fundamental studies and laser designs.

It is important to point out that the circulating (or longitudinal) modes in the laser cavity discussed here resemble those in microdisk lasers. However, the modes shown in Fig. 2 are well-defined rather than having a chaotic nature. Unlike microdisk lasers, light output couplings here are not much different from conventional stripe laser diodes.

IV. CONCLUSIONS

In summary, we have established a method for analytically calculating the TM modes inside equilateral triangular laser cavities. Recently, this method has been successfully applied to TE modes and to modes in hexagonal cavities, again all in analytical form, and will be presented elsewhere. The cavities can be easily fabricated by cleaving samples grown on (111) substrates. The technique is very similar to that for conventional edge emitting, cleaved cavities of broad-area laser structures, both in simplicity of the procedure and in the high quality of the cleaved facets. The design can be used for all commonly studied semiconductor material systems grown on (111) substrates.

ACKNOWLEDGMENTS

The authors benefited from discussions with B. D. McCombe and the use of his laboratories for fabricating the laser cavities. The project was supported by the Center for Advanced Photonic and Electronic Materials at SUNY-Buffalo.

[1] K. Iga, F. Koyama, and S. Kinoshita, IEEE J. Quantum Electron. **24**, 1845 (1988).
[2] S. L. McCall, A. F. J. Levi, R. E. Slusher, S. J. Pearton, and R. A. Logan, Appl. Phys. Lett. **60**, 289 (1992).
[3] S. Mitsugi, J. Kato, F. Koyama, A. Matsutani, T. Mukaihara, and K. Iga, Jpn. J. Appl. Phys., Part 1 **33**, 6201 (1994).
[4] A. Behfar-Rad, J. M. Ballantyne, and S. S. Wong, Appl. Phys. Lett. **59**, 1395 (1991).
[5] A. Behfar-Rad, S. S. Wong, J. M. Ballantyne, B. A. Soltz, and C. M. Harding, Appl. Phys. Lett. **54**, 4931 (1989).
[6] F. Shimokawa, H. Tanaka, R. Sawada, and S. Hara, Appl. Phys. Lett. **56**, 1617 (1990).
[7] C. Gmachl, F. Capasso, E. E. Narimanov, J. U. Nkel, A. D. Stone, J. Faist, D. L. Sivco, and A. Y. Cho, Science **280**, 1556 (1998).
[8] M. Asif Khan, Q. Chen, J. Yang, C. J. Sun, B. Lim, H. Temkin, J. Schetzina, and M. S. Shur, Mater. Sci. Eng., B **43**, 265 (1997).
[9] S. Bidnyk, B. D. Little, Y. H. Cho, J. Krasinski, J. J. Song, W. Yang, and S. A. McPherson, Appl. Phys. Lett. **73**, 2242 (1998).
[10] E. A. Khoo, A. S. Pabla, J. Woodhead, J. P. R. David, R. Grey, and G. J. Rees, Electron. Lett. **33**, 957 (1997).
[11] S. Ando, N. Kobayashi, and H. Ando, Jpn. J. Appl. Phys., Part 2 **35**, L411 (1996); **36**, L76 (1997).
[12] J. C. Marinace, A. E. Michel, and M. I. Nathan, Proc. IEEE **55**, 722 (1964).
[13] See, for example, J. D. Jackson, *Classical Electrodynamics*, 2nd ed. (John Wiley & Sons, New York, 1975), Chap. 8.
[14] See, for example, C. Itzykson and J. M. Luck, J. Phys. A **19**, 211 (1986).
[15] M. I. Nathan, A. B. Fowler, and G. Burns, Phys. Rev. Lett. **11**, 152 (1963).
[16] D. T. F. Marple, J. Appl. Phys. **35**, 1241 (1964).